Available online at www.sciencedirect.com
ScienceDirect
C. R. Physique 10 (2009) 216–226
COMPTES RENDUS PHYSIQUE

Laser acceleration of particles in plasmas / Accélération laser de particules dans les plasmas

On the ion acceleration by high power electromagnetic waves in the radiation pressure dominated regime

Sergei V. Bulanov [a,b,*], Timur Zh. Esirkepov [a], Francesco Pegoraro [c], Marco Borghesi [d]

[a] *Advanced Photon Research Center, JAEA, 8-1 Umemidai, Kizugawa, 619-0215 Kyoto, Japan*
[b] *A.M. Prokhorov Institute of General Physics, RAS, Vavilov street, 38, 119991 Moscow, Russia*
[c] *Physics Department and CNISM, University of Pisa, Largo Pontecorvo, 3, 56127 Pisa, Italy*
[d] *School of Mathematics and Physics, The Queen's University of Belfast, Belfast, Northern Ireland, UK*

Available online 29 April 2009

Abstract

When the laser pulse radiation pressure is dominant, the efficiency of the laser energy transformation into the energy of relativistic ions is very high. An analysis of the stability of a thin plasma slab accelerated by the radiation pressure shows that the onset of a Rayleigh–Taylor-like instability can lead to transverse bunching of the slab. At the nonlinear stage of the instability development the plasma slab breaks up into separated clumps, which are accelerated by the wave radiation pressure. An indication of the effect of radiation pressure on the bulk target ions is obtained in the experimental studies of plasma jets ejected from the rear side of thin solid targets irradiated by ultraintense laser pulses. ***To cite this article: S.V. Bulanov et al., C. R. Physique 10 (2009).***

Résumé

Sur l'accélération d'ions par des ondes électromagnétiques de haute intensité dans le régime dominé par la pression de radiation. Quand la pression de radiation laser est dominante, l'efficacité de la transformation de l'énergie laser en énergie des ions relativistes est élevée. Une analyse de la stabilité d'une mince tranche de plasma accélérée par la pression de rayonnement montre que le déclenchement d'une instabilité du type Rayleigh–Taylor peut mener à un fractionnement transverse de la tranche. Dans la phase nonlinéaire de développement de l'instabilité la tranche se divise en morceaux séparés, qui sont accélérés par la pression de rayonnement de l'onde. Une indication de l'effet de la pression de rayonnement sur les ions de la cible est obtenue dans des études expérimentales de jets de plasma éjectés de la face arrière de cibles minces solides irradiées par des impulsions ultra-intenses. ***Pour citer cet article : S.V. Bulanov et al., C. R. Physique 10 (2009).***

Keywords: Relativistic laser plasmas; Charged particle acceleration; Radiation pressure dominated acceleration

Mots-clés : Plasmas laser relativistes ; Accélération de particules chargées ; Accélération dominée par la pression de rayonnement

* Corresponding author.
E-mail address: bulanov.sergei@jaea.go.jp (S.V. Bulanov).

1631-0705/$ – see front matter
doi:10.1016/j.crhy.2009.03.001

1. Introduction

Ion acceleration by a high intensity electromagnetic wave incident on an electron cloud carrying a small portion of ions was proposed by V.I. Veksler more than 50 years ago [1]. In this mechanism the ion acceleration occurs in the collective electric field which is produced due to the radiation pressure acting on the electron component. Laser-driven fast ions are considered in regard to a broad range of applications (see review articles [2,3]).

The transition to powers of electromagnetic radiation corresponding to relativistically strong fields radically changes the acceleration regime. In Ref. [4], a regime where the ion acceleration in a plasma is directly due to the radiation pressure of the electromagnetic wave has been identified. In this radiation pressure dominant acceleration (RPDA) regime (it is equivalently called the "Laser Piston"), the ions move forward with almost the same velocity as the electrons and thus have a kinetic energy well above that of the electrons. This acceleration process is highly efficient with the ion energy per nucleon being proportional to the electromagnetic pulse energy. This acceleration mechanism has attracted a great deal of attention. In Ref. [5] the stability of the accelerated foil has been analyzed. Refs. [6] are devoted to extending its range operation towards lower electromagnetic wave intensities. In Ref. [4] it has been shown that a foil interacting with a laser pulse becomes deformed and changes into a "cocoon", which, in turn, traps the electromagnetic wave, thus allowing the ion acceleration over a distance larger than the Rayleigh length. The leading edge of the cocoon moves at a relativistic speed.

In the present paper we discuss the ion acceleration mechanism when the ion-electron thin foil is accelerated by the radiation pressure of a high intensity electromagnetic wave. We consider the foil stability and the effects of the foil expansion in the transverse direction. At the end of the article we discuss the results of experiments [7] that appear consistent with Radiation Pressure effects.

2. Mathematical model

We generalize the results obtained in Refs. [4,5]. In the electromagnetic wave interaction with the foil, the latter is modeled as an ideally reflecting mirror. The equations of motion of the surface element $|\mathrm{d}\sigma|$ of an ideally reflecting mirror in the laboratory frame of reference can be written in the form

$$\frac{\mathrm{d}p_i}{\mathrm{d}t} = \mathcal{P}\,\mathrm{d}\sigma_i \tag{1}$$

where $p_i = (p_x, p_y, p_z)$ is the momentum of the mirror surface element, $\mathrm{d}\sigma_i$ is a vector normal to the mirror surface, $i = 1, 2, 3$, and $\mathcal{P}$ is equal to the relativistically invariant pressure.

We consider a configuration where the electromagnetic wave propagates along the x axis and the initial position of the mirror is in the plane y, z. In the co-moving frame of reference the radiation pressure $\mathcal{P}$ for normal wave incidence is given by expression $\mathcal{P} = E_M^2/2\pi$, where E_M is the electric field amplitude. In the laboratory frame of reference we have $E_M^2 = (\omega_M/\omega_0)^2 E_0^2$ with ω_M and ω_0 being the frequency values in the co-moving and in the laboratory frames of reference. For ω_M and ω_0 we have the relationship $\omega_M = \omega_0[(1-\beta)/(1+\beta)]^{1/2}$.

As is well known, an approach towards the description of the problem of nonlinear regimes of the Raleigh–Taylor instability of a thin foil has been formulated in Ref. [8] and further developed in a number of publications, e.g. see Refs. [9]. We consider a thin plane shell with surface particle number equal to $n_0 l_0$, where l_0 is the shell thickness. At the initial time the shell is at rest in the plane $x = 0$. In order to derive the equations of shell motion we introduce the Lagrange coordinates η and ζ, related to the Euler coordinates x, y, z as $x_i = x_{0,i} + \xi_i(\mathbf{x}_0, t)$, with $x_{0,i} = (0, \eta, \zeta)$ and the displacements $\xi_i(\mathbf{x}_0, t)$. The velocity of the surface element is given by $v_i = \partial_t \xi_i$. At $t = 0$ we have $\xi_i(\mathbf{x}_0, 0) = 0$ and $\partial_t \xi_i(\mathbf{x}_0, t) = v_i(\mathbf{x}_0, 0)$. Here the Lagrange coordinates η and ζ mark the element of the shell surface. Initially, at $t = 0$ the coordinates of the shell element $\mathrm{d}\boldsymbol{\sigma}$ center $\mathrm{d}\boldsymbol{\sigma}_0$ are $(0, \eta, \zeta)$. At time t it is located at the point with coordinates x, y, z. Due to the conservation of the number of particles in the shell element, $\mathrm{d}N = n_0 l_0 |\mathrm{d}\boldsymbol{\sigma}_0| = \text{constant}$, we have the relationship

$$v_0 |\mathrm{d}\boldsymbol{\sigma}_0| = v |\mathrm{d}\boldsymbol{\sigma}| \tag{2}$$

where $v_0 = n_0 l_0$ and $v = nl$. Writing $\mathrm{d}\boldsymbol{\sigma}_0$ and $\mathrm{d}\boldsymbol{\sigma}$ in terms of the Lagrange and Euler coordinates we obtain $|\mathrm{d}\boldsymbol{\sigma}_0| = |\mathrm{d}\boldsymbol{\eta} \times \mathrm{d}\boldsymbol{\zeta}|$ and $|\mathrm{d}\boldsymbol{\sigma}| = |\mathrm{d}\mathbf{y} \times \mathrm{d}\mathbf{z}, \mathrm{d}\mathbf{z} \times \mathrm{d}\mathbf{x}, \mathrm{d}\mathbf{x} \times \mathrm{d}\mathbf{y}|$. Here $\mathrm{d}\mathbf{x}, \mathrm{d}\mathbf{y}, \mathrm{d}\mathbf{z}$ are the vectors of the length $|\mathrm{d}\mathbf{x}|, |\mathrm{d}\mathbf{y}|, |\mathrm{d}\mathbf{z}|$, directed along the axes x, y, z.

Using Eq. (2), we find a relationship between the values of the surface density at time $t = 0$ and t:

$$\nu = \nu_0 \left| \frac{\mathrm{d}\boldsymbol{\sigma}_0}{\mathrm{d}\boldsymbol{\sigma}} \right| = \frac{\nu_0}{[\{y,z\}^2 + \{z,x\}^2 + \{x,y\}^2]^{1/2}} \tag{3}$$

where $\{x_j, x_k\}$ are the Poisson brackets defined as $\{x_j, x_k\} = \partial_\eta x_j \partial_\zeta x_k - \partial_\zeta x_j \partial_\eta x_k$.

With the help of Eqs. (1) and (3) we obtain the equations of motion for the shell element

$$\partial_t p_i = \frac{\mathcal{P}}{\nu_0}\{x_{0,j} + \xi_j, x_{0,k} + \xi_k\}, \quad \partial_t \xi_i = c\frac{p_i}{(M_\alpha^2 c^2 + p_k p_k)^{1/2}} \tag{4}$$

where M_α is the ion mass. Here and below the indices i, j, k are pairwise different.

3. RPDA ion acceleration

3.1. RPDA regime of the ion acceleration during interaction of electromagnetic pulse with a thin shell which is at rest at the initial time

Assuming that the foil moves along the x axis, i.e. that the initial conditions define a plane mirror homogeneous along the y and z directions, and $y^{(0)} = \eta$, $z^{(0)} = \zeta$, i.e. $\xi_x = 0$ and $\xi_y = 0$ we can represent the x-component of Eq. (4) in the form

$$\frac{\mathrm{d}p_x^{(0)}}{\mathrm{d}t} = \frac{E_0^2}{2\pi\nu_0}\frac{M_\alpha c\gamma^{(0)} - p_x^{(0)}}{M_\alpha c\gamma^{(0)} + p_x^{(0)}} \tag{5}$$

where $p_x^{(0)}$ depends only on time t. The relativistic gamma-factor is equal to

$$\gamma^{(0)} = \left(1 + \left(p_x^{(0)}/M_\alpha c\right)^2\right)^{1/2}$$

The solution of Eq. (5) is formally equivalent to the solution of the problem of charged particle motion under the radiation pressure of electromagnetic wave presented in "The Classical Theory of Fields" by L.D. Landau and E.M. Lifshitz (see Problem 7 in Section 78 in [10]). If the initial value of the particle momentum vanishes, $p_x^{(0)}(0) = 0$, the dependence of the particle momentum on time $p_x^{(0)}(t)$ for a constant amplitude of electromagnetic wave $E_0^2 = \text{constant}$, can be written as

$$p_x^{(0)}(\tau) = \frac{M_\alpha c}{4(2+3\tau)}\left\{\left[47 + 8(2+3\tau)\left(5+3\tau(4+3\tau)\right)^{3/2} + 12\tau(4+3\tau)\left(11+6\tau(4+3\tau)\right)\right]^{1/3} - 1 \right.$$
$$\left. - \frac{31 + 24\tau(4+3\tau)}{[47 + 8(2+3\tau)(5+3\tau(4+3\tau))^{3/2} + 12\tau(4+3\tau)(11+6\tau(4+3\tau))]^{1/3}}\right\} \tag{6}$$

where $\tau = E_0^2 t/2\pi\nu_0 M_\alpha c$ is a normalized time. We note that more compact form of the solution of the problem of foil element motion under the radiation pressure of electromagnetic wave has been obtained in Ref. [4] with the dependence of the momentum on time written in terms of hyperbolic functions. The above presented dependence given by Eq. (6) is explicit. In the limit $\tau \to \infty$ we have

$$p_x^{(0)}(\tau)/M_\alpha c = (3\tau/4)^{1/3} - (6/\tau)^{1/3} + \cdots \tag{7}$$

In the case of a finite length electromagnetic pulse the electric field E_0 value at the moving shell, i.e. at $x = x(t)$, depends on time as $E_0(t - x(t)/c)$. The function $x(t)$ must be found from Eqs. (4). We introduce new variable

$$\psi = \omega_0\left(t - x^{(0)}(t)/c\right) \tag{8}$$

equal to the phase of the wave at the shell, $x = x^{(0)}(t)$. Differentiating Eq. (8) with respect to time, we find

$$\frac{\mathrm{d}\psi}{\mathrm{d}t} = \omega_0\frac{M_\alpha c\gamma^{(0)} - p_x^{(0)}}{M_\alpha c\gamma^{(0)}} \tag{9}$$

Changing from the variable t to ψ and introducing normalized fluence of electromagnetic wave, which is the energy flux per unit surface,

$$w(\psi) = \int_0^{\psi} \frac{R(\psi')}{2\lambda_0}\,\mathrm{d}\psi' \tag{10}$$

where $R(\psi) = E_0^2(\psi)/M_\alpha \nu_0 \omega_0^2$ and $\lambda_0 = 2\pi c/\omega_0$, we can find the solution to Eq. (5). If the initial value of the momentum vanishes, $p_x^{(0)}(0) = 0$, the solution takes the form

$$p_x^{(0)}(\psi) = M_\alpha c \frac{2w(\psi)(w(\psi)+1)}{2w(\psi)+1} \tag{11}$$

Eq. (9) yields a relationship between the variables t and ψ:

$$\psi + \int_0^{\psi} \left[2w(\psi') + w(\psi')^2\right]\mathrm{d}\psi' = \omega_0 t \tag{12}$$

In the case of constant amplitude electromagnetic wave, when $R = R_0 = E_0^2/2M_\alpha \nu_0 \omega_0^2$, expressions (10) and (12) give $w(\psi) = (R_0/\lambda_0)\psi$ and $3\psi + 3(R_0/\lambda_0)\psi^2 + 2(R_0/\lambda_0)^2\psi^3 = 3\omega_0 t$. The x component of the shell element momentum $p_x^{(0)}$ in the limit $t \gg \omega_0^{-1}(\lambda_0/R_0)$ depends on time as

$$p_x^{(0)} \approx M_\alpha c(3R_0\omega_0 t/\lambda_0)^{1/3} \tag{13}$$

in accordance with expression (7).

We note that the dependence $t^{1/3}$ of the fast ion energy on time has been observed in the 3D computer simulations of thin shell acceleration by super strong electromagnetic pulse (see Ref. [4]). From expression (11) it follows that the efficiency of the electromagnetic wave energy transformation into the energy of fast ions (this efficiency is defined as $\kappa_{eff} = (\gamma^{(0)} - 1)/w$) tends to unity for $w \to \infty$.

3.2. RPDA ion acceleration when the electromagnetic wave interacts with the shell expanding or contracting in the transverse direction

We assumed above that the transverse coordinates of the shell element do not depend on time, $y^{(0)} = \eta$ and $z^{(0)} = \zeta$. In the general case the shell can expand or contract in the transverse direction. We shall take into account the transverse expansion (contraction) of the shell assuming the transverse motion to be nonrelativistic similarly to the approximation used in accelerator theory [11].

3.2.1. Nonrelativistic limit

If at first we consider the nonrelativistic limit for the longitudinal motion, Eqs. (4) can be written as

$$\partial_{tt}\xi_i = \frac{\mathcal{P}}{M_\alpha \nu_0}\{x_{0,j} + \xi_j, x_{0,k} + \xi_k\} \tag{14}$$

In the simplest case, which corresponds to a local approximation in the vicinity of the electromagnetic pulse axis, the shell expansion (contraction) is uniform in the y, z plane. We present a dependence between the Lagrange and the Euler variables of the form $\xi_x = \xi_x^{(0)}(t)$, $\xi_y = m_y^{(0)}(t)\eta$, $\xi_z = m_z^{(0)}(t)\zeta$ and substitute it into Eqs. (4), taking into account the smallness of the transverse components of momentum with respect to the longitudinal one. We choose the initial conditions for the deformation parameters, $m_y^{(0)}$ and $m_z^{(0)}$, for which $m_y^{(0)}(0) = 0$, $\dot{m}_y^{(0)}(0) = \omega_y^{(0)}$, $m_z^{(0)}(0) = 0$, and $\dot{m}_z^{(0)}(0) = \omega_z^{(0)}$. As a result, the y- and z-components of Eqs. (14) yield the following expressions for the transverse coordinates of the shell element,

$$y^{(0)}(t) = \left(1 + \omega_y^{(0)} t\right)\eta, \quad z^{(0)}(t) = \left(1 + \omega_z^{(0)} t\right)\zeta \tag{15}$$

in which case the surface density, $\nu(t)$, depends on time. According to Eq. (3) we have

$$\nu(t) = \frac{\nu_0}{|\{y, z\}|} = \frac{\nu_0}{|(1 + \omega_y^{(0)} t)(1 + \omega_z^{(0)} t)|} \tag{16}$$

If the parameters $\omega_y^{(0)}$ and $\omega_z^{(0)}$ do not vanish and are positive, the surface density decreases: for $t \to \infty$ we have $\nu(t) \propto 1/t^2$. For negative values of one or both the parameters $\omega_y^{(0)}$ and/or $\omega_z^{(0)}$ the surface density $\nu(t)$ becomes equal to infinity in a finite interval of time,

$$t_{coll} = 1/\max\{|\omega_y^{(0)}|, |\omega_z^{(0)}|\} \tag{17}$$

This case corresponds to the singularity formation.

Substituting the dependence given by Eq. (16) into Eqs. (14), we find the equation for the x component of the momentum

$$\frac{\mathrm{d}^2\xi_x^{(0)}}{\mathrm{d}t^2} = \frac{\mathcal{P}}{M_\alpha \nu_0}\left(1+\omega_y^{(0)}t\right)\left(1+\omega_z^{(0)}t\right) \tag{18}$$

Its solution in the case of a constant amplitude electromagnetic wave, $E_0^2 = \text{constant}$, is given by

$$\xi_x^{(0)}(t) = \frac{\mathcal{P}}{6\nu_0 M_\alpha} t^2\left[6 + 2\left(\omega_y^{(0)} + \omega_z^{(0)}\right)t + \omega_y^{(0)}\omega_z^{(0)}t^2\right] \tag{19}$$

For positive parameters $\omega_y^{(0)}$ and $\omega_z^{(0)}$ from the equation (19) it follows that asymptotically at $t \to \infty$ the longitudinal component of the momentum $p_x^{(0)}$ depends on time as

$$p_x^{(0)} \approx M_\alpha c\left(\frac{2\mathcal{P}}{3\nu_0 M_\alpha c}\omega_y^{(0)}\omega_z^{(0)}\right)t^3 \tag{20}$$

i.e. the kinetic energy grows proportionally to t^6.

3.2.2. Ultrarelativistic case

Here we assume that $p_x^{(0)}/M_\alpha c \gg 1$ and $p_y/p_x^{(0)} \ll 1$ and $p_z/p_x^{(0)} \ll 1$. Using this approximation we find instead of Eq. (15)

$$y^{(0)}(t) = \left(1 + \int_0^t \frac{\pi_y^{(0)}}{M_\alpha \gamma^{(0)}(t')}\,\mathrm{d}t'\right)\eta \quad \text{and} \quad z^{(0)}(t) = \left(1 + \int_0^t \frac{\pi_z^{(0)}}{M_\alpha \gamma^{(0)}(t')}\,\mathrm{d}t'\right)\zeta \tag{21}$$

where $\pi_y^{(0)}$ and $\pi_z^{(0)}$ are related to the initial components of transverse momentum, $p_y^{(0)}$ and $p_z^{(0)}$, as $p_y^{(0)} = \pi_y^{(0)}\eta$ and $p_z^{(0)} = \pi_z^{(0)}\zeta$. The transverse momentum components, $p_y^{(0)}$ and $p_z^{(0)}$, are determined by the initial conditions and by

$$\gamma^{(0)}(t) = \left(1 + \left(p_x^{(0)}(t)/M_i c\right)^2\right)^{1/2}$$

Substitution of the relationships (21) into Eqs. (4) yields

$$\frac{\mathrm{d}p_x^{(0)}}{\mathrm{d}t} = \frac{\mathcal{P}\pi_y^{(0)}\pi_z^{(0)}c^2}{4\nu_0 M_\alpha^2}\frac{M_\alpha c\gamma^{(0)} - p_x^{(0)}}{M_\alpha c\gamma^{(0)} + p_x^{(0)}}\left(\int_0^t \frac{\mathrm{d}t'}{\gamma^{(0)}(t')}\right)^2 \tag{22}$$

The asymptotic solution for $\pi_y^{(0)} > 0$ and $\pi_z^{(0)} > 0$ gives the following time dependence of $p_x^{(0)}(t)$:

$$p_x^{(0)}(t) \approx \left(125\mathcal{P}\pi_y^{(0)}\pi_z^{(0)}c^2/48\nu_0\right)^{1/5}t^{3/5} \tag{23}$$

We see that in the case of expanding foil the acceleration efficiency is higher than in the case of the foil which does not expand in the transverse direction.

We note that for contracting foil with $\pi_y^{(0)} < 0$ and/or $\pi_z^{(0)} < 0$ ($\omega_y^{(0)} < 0$ and/or $\omega_z^{(0)} < 0$ in the nonrelativistic limit) the density becomes infinite in a finite time (17) and the acceleration stops.

4. Instability of a thin shell accelerated by the radiation pressure of electromagnetic wave

Now we consider the problem of the stability of the accelerated shell with respect to perturbations $\xi_i^{(1)}(\mathbf{x}_0, t)$, resulting in the shell deformations in the transverse direction. Linearizing the system (4) around the unperturbed solution given by Eq. (10), we obtain

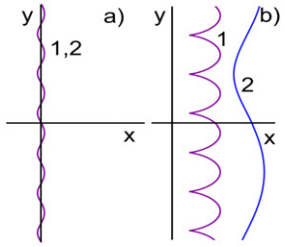

Fig. 1. Growth of nonlinear perturbations (1) for a not expanding foil with $\tilde{\omega}_x = 0$ and (2) for a foil expanding in the transverse direction with $\tilde{\omega}_x = 1$. Foil shape at $\tilde{\tau} = 0$ (a) and at $\tilde{\tau} = 4$ (b) for $\rho = 0.5$, $q = 0.25$.

$$\partial_{\psi\psi}\xi_x^{(1)} + \frac{\partial_\psi p_x^{(0)}}{p_x^{(0)}}\partial_\psi \xi_x^{(1)} = \frac{R(\psi)M_\alpha c}{2\pi p_x^{(0)}}\left(\partial_\eta \xi_y^{(1)} + \partial_\zeta \xi_z^{(1)}\right) \tag{24}$$

$$\partial_{\psi\psi}\xi_y^{(1)} - \frac{\partial_\psi p_x^{(0)}}{p_x^{(0)2}}\partial_\psi \xi_y^{(1)} = -\frac{R(\psi)p_x^{(0)}}{2\pi M_\alpha c}\partial_\eta \xi_x^{(1)} \tag{25}$$

$$\partial_{\psi\psi}\xi_z^{(1)} - \frac{\partial_\psi p_x^{(0)}}{p_x^{(0)2}}\partial_\psi \xi_z^{(1)} = -\frac{R(\psi)p_x^{(0)}}{2\pi M_\alpha c}\partial_\zeta \xi_x^{(1)} \tag{26}$$

Using the ultra-relativistic approximation, $p_x^{(0)}/M_i c \gg 1$, in these equations we keep leading only the terms.

We seek the solution to Eqs. (24)–(26) in the WKB approximation and represent the functions $\xi_i^{(1)}(\eta, \zeta, \psi)$ in the form

$$\xi_i^{(1)}(\eta, \zeta, \psi) \propto \exp\left(\int_0^\psi \Gamma(\psi')\,\mathrm{d}\psi' - iq\eta - ir\zeta\right) \tag{27}$$

under the condition of a slow dependence of the growth rate Γ on the variable ψ: $\partial_\psi \Gamma/\Gamma^2 \ll 1$. Substituting expression (27) into Eqs. (24)–(26), we find

$$\Gamma(\psi) = \left(q^2 + r^2\right)^{1/4}\left(R(\psi)/2\pi\right)^{1/2} \tag{28}$$

with $\xi_x^{(1)} \approx (M_\alpha c/p_x^{(0)})\xi_y^{(1)} \approx (M_\alpha c/p_x^{(0)})\xi_z^{(1)}$. In two-dimensional geometry this expression reduces to the expression found in Ref. [5]. Using relationships (13) we find for the case of a constant amplitude electromagnetic wave that the perturbations depend on time as

$$\xi_i^{(1)}(\eta, \zeta, t) \propto \exp\left((t/\tau_r)^{1/3} - iq\eta - ir\zeta\right) \tag{29}$$

where the characteristic timescale of the instability development in the ultrarelativistic limit is equal to $\tau_r = \omega_0^{-1}[(2\pi)^{3/2}R_0^{1/2}]/[6(q^2 + r^2)^{3/4}\lambda_0^2]$.

Taking into account that $R_0 = E_0^2/M_\alpha \nu_0 \omega_0^2$ we see that the instability timescale is proportional to the square root of the ratio of the radiation pressure to the ion mass. In other words, the higher the ion mass the faster the instability develops and the larger the radiation pressure the slower the perturbations grow.

It is easy to show, that in the nonrelativistic limit the perturbations depend on time and on the Lagrange coordinates, η and ζ, as

$$\xi_i^{(1)}(\eta, \zeta, t) \propto \exp(t/\tau_{nr} - iq\eta - ir\zeta) \tag{30}$$

where the characteristic timescale of the instability is $\tau_{nr} = \omega_0^{-1}(2\pi/R_0)^{1/2}(q^2 + r^2)^{-1/4}$.

4.1. Effect of the shell stretching on the R-T instability

The plasma expansion along the foil surface may result in the slow-down of onset of the nonlinear stage of instability with the cusps, the plasma clumps, formation.

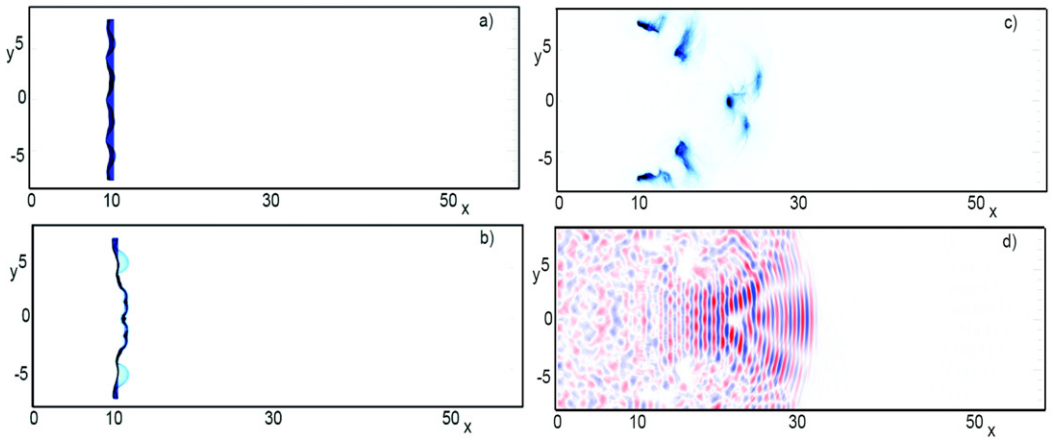

Fig. 2. (a)–(c) Proton density distribution in the x–y plane at $t = 40$, 50, 70, respectively; (d) laser pulse electric field $E_z(x, y)$ at $t = 70$.

If at first we consider the nonrelativistic limit for the longitudinal motion, and seek for the sake of simplicity two dimensional solutions to Eqs. (14) of the form

$$\xi_x(\eta, t) = \xi_x^{(0)}(t) + \xi_x^{(2)}(\eta, t), \quad \xi_y(\eta, t) = \xi_y^{(1)}\omega_y t\eta + \xi_y^{(2)}(\eta, t), \quad \xi_z = 0 \tag{31}$$

Substituting these expressions into Eqs. (14) we find

$$\xi_x(\eta, \tilde{\tau}) = \tilde{\tau}^2/2 + \tilde{\omega}_y^3\tilde{\tau}/6 - \rho\exp(\sqrt{q}\tilde{\tau})\sin(q\eta) \tag{32}$$

$$\xi_y(\eta, \tilde{\tau}) = \tilde{\omega}_y\tilde{\tau}\eta + \rho\exp(\sqrt{q}\tilde{\tau})\cos(q\eta) \tag{33}$$

where $\tilde{\tau} = t(\mathcal{P}/v_0)^{1/2}$ and $\tilde{\omega}_y = \omega_y(v_0/\mathcal{P})^{1/2}$.

These expressions describe the time evolution of the foil form as it is shown in Fig. 1. We see that instability evolves into the nonlinear regime faster in the not-expanding foil reaching the stage when the cusp are formed at $\tilde{\tau} = 4$ for the amplitude and wave number of initial perturbations equal to $\rho = 0.5$ and $q = 0.25$, while the stretching results in the growth of the perturbation wavelength in the expanding foil.

5. Computer simulation of the R-T instability development of a premodulated shell

In order to investigate the onset and the nonlinear evolution of the instability of the foil, we have performed a numerical simulation using the 2D version of the PIC e.m. relativistic code REMP, see Ref. [12]. The size of the computation box is $60\lambda \times 15\lambda$ with a mesh of 80 cells per laser wavelength λ. The total number of quasiparticles in the plasma region is equal to 2×10^7. A thin plasma slab, of width 12.5λ and thickness 1λ, is localized at $x = 10\lambda$. The plasma is made of fully ionized hydrogen ions; the ion to electron mass ratio is 1836. The electron density corresponds to the ratio $\omega_{pe}/\omega = 10$. An s-polarized pulse with electric field along the z-axis is initialized in vacuum at the left-hand side of the plasma slab. The pulse has a form given by

$$a_0 \times \left[\exp\left(-\frac{(x - 2.5l_x)^2}{2l_x^2} - \frac{y^2}{2l_y^2}\right) + 0.125\exp\left(-\frac{2x^2}{l_x^2}\right)\sin\left(\frac{8y}{l_y}\right)\right] \tag{34}$$

with $l_x = 20\lambda$, $l_y = 12.5\lambda$. It is a superposition of a "Gaussian" pulse and relatively weak sinusoidal in the y-direction modulations. The pulse dimensionless amplitude, $a_0 = 160$, corresponds for $\lambda = 1$ μm to the intensity $I \approx 3.5 \times 10^{22}$ W/cm^2 ($R_{max}/\lambda_0 = 27.5$).

The results of these simulations are shown in Figs. 2–4. The wavelength λ of the incident radiation and its period $2\pi/\omega$ are chosen as units of length and time. The distribution in the x–y plane of the proton density and of the laser pulse electric field are shown in frames from (a) to (c) at $t = 40$, 50, 70, respectively.

In Fig. 2(a), we see the periodically premodulated shell. Fig. 2(b) shows an initial stage of the R-T instability: the instability develops with a growth rate of several tens of inverse laser periods, consistent with the analytical estimate $\omega_0/\tau_r < 1$, with the formation of cusps and of multiple bubbles in the plasma density distribution. In the

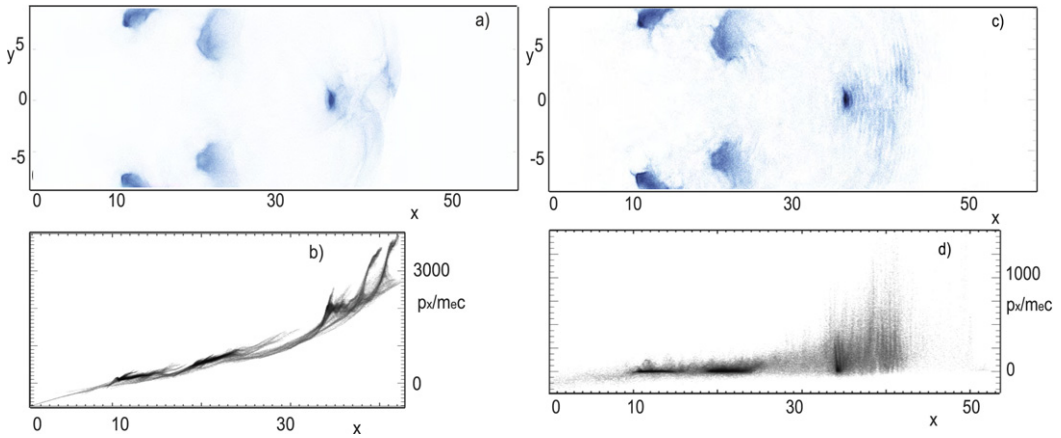

Fig. 3. (a) Proton density distribution in the x–y plane and (b) the proton phase plane at $t = 90$; (c) electron density distribution in the x–y plane and (d) the electron phase plane at $t = 90$.

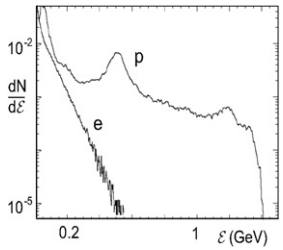

Fig. 4. Proton and electron energy spectrum at $t = 100$.

nonlinear stage, we see the formation of relatively large scale clump bubbles. The laser electric field is modulated in the longitudinal and transverse directions as seen in Fig. 2(c). The protons are accelerated forward, and their spectrum consists of quasimonoenergetic beamlets, shown in Figs. 3 and 4, where we present the proton, Fig. 3(a), and electron, Fig. 3(c), density distribution at $t = 90$. In frames Figs. 3(b) and 3(d) we show the proton and electron phase planes, x, p_x, respectively. Fig. 4 shows the proton and electron energy spectra at $t = 100$.

In Fig. 3, the fully nonlinear stage of the instability results in the formation of several clumps in the proton density distribution, moving with relativistic velocities, with more diffuse, lower density plasma clouds between them. The high-energy tail in the proton spectrum (Fig. 4) grows much faster than in the stable case. The local maxima at relatively lower energy correspond to the plasma clumps. When the instability develops from noise, the clumps in the instability nonlinear stage propagate at different angles, but remain well collimated in the forward direction close to the axis (see Ref. [5] and Fig. 3 therein). As we have seen above more collimated clumps can be obtained using shaped laser pulses.

6. Experimental evidence of plasma jets driven by ultraintense-laser interaction with thin foils

Although at moderate laser light intensity the ion acceleration mechanism due to the charge separation at the rear target surface and the ion acceleration at the front of a plasma expanding into vacuum will be the dominant process leading to high-energy acceleration, radiation pressure can still play a significant role by driving the ions from the front-surface into the target and forming plasma jets at the rear side. Results published in Refs. [3,7] suggest that this process can lead to the ejection of well-collimated plasma jets, when the accelerated ion bunches break out at the rear surface of thin foils. Fig. 5 shows interferograms obtained at the VULCAN facility at the Rutherford Appleton laboratory, where the target was irradiated at intensities in the range from 3×10^{19} to 5×10^{20} W/cm^2. While in thin targets (5 μm targets) there is a clearly evident plasma jet expanding from the target, with increasing thickness the plasma profile presents the features of an ordinary thermal plasma expansion.

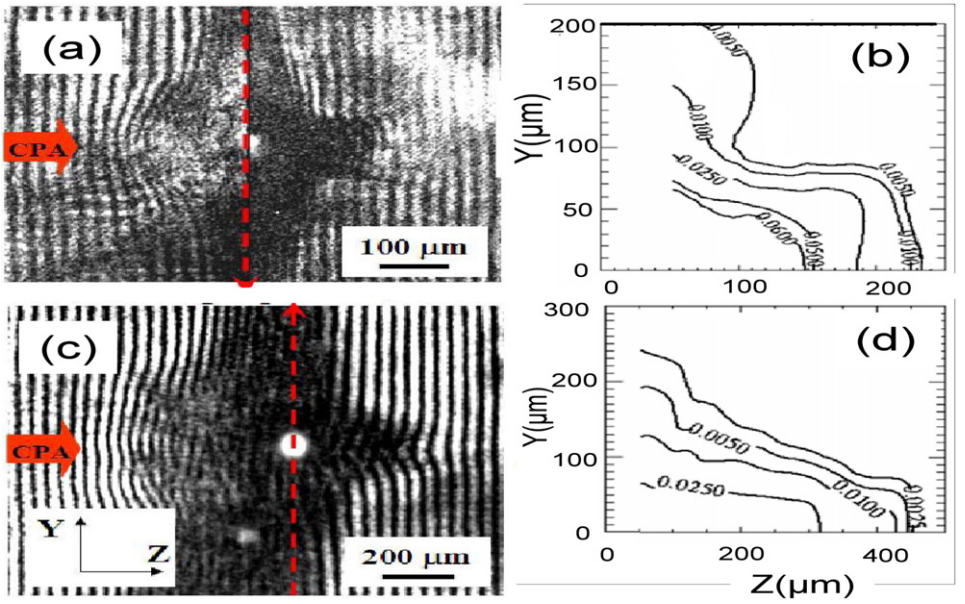

Fig. 5. Interferograms of laser-irradiated foils showing jet formation at the target rear: (a) 3 μm Al foil irradiated by 1 ps pulse at 3×10^{19} W/cm^2; (c) 5 μm Cu foil irradiated by a 700 fs pulse 10^{20} W/cm^2. Probing time: (a) +250 ps; (c) +400 ps after the arrival of the CPA on target. The inverted electron density profile contour plots (in the unit of 10^{21} cm^{-3}) of the rear side plasma are shown next to the respective interferograms [(b), (d)].

Numerical simulations [7] suggest that radiation pressure plays an important role in the formation of these jets. In order to explain the observed longitudinal velocity achieved by the plasma jet, we considered a piston-like push of the portion of the target that has been irradiated by the laser pulse. Within the framework of the one-dimensional snowplow approximation, we can write the equation of motion of the plasma (in nonrelativistic approximation) as

$$\frac{\mathrm{d}}{\mathrm{d}t}\left(M_\alpha \nu(x)\frac{\mathrm{d}x}{\mathrm{d}t}\right) = \mathcal{P} \tag{35}$$

which has a form of the Meshchersky equation. Here $\nu(x) = \int_0^x n_0(s)\,\mathrm{d}s$ with $n_0(x)$ the ion density distribution inside the foil. For short laser pulse with duration $\tau_{las} < l_0/\Delta v_\alpha$, where l_0 and Δv_α are the foil thickness and the ion velocity, we obtain $v_\alpha(t) = (\mathcal{P}\tau_{las}/2M_\alpha n_0)^{1/2} t^{-1/2}$ and $\Delta v_\alpha = (\mathcal{P}\tau_{las}/M_\alpha n_0 l_0)$. The efficiency of the laser energy transformation into the kinetic energy of fast ions is $\kappa_{eff} = \mathcal{E}_\alpha/\mathcal{E}_{las} = (\Delta v_\alpha/c)^2$. For long laser pulse with $\tau_{las} > l_0/\Delta v_\alpha$, the ion momentum is given by Eq. (11). In the nonrelativistic limit when $w \ll 1$, $\mathcal{E}_\alpha = 2M_\alpha c^2 w^2$ and $\kappa_{eff} = 2w$. According to the above expressions, the axial velocity of the jet emerging from a displaced Al foil ($n_0 \approx 60 n_{cr}$) at a laser irradiance of 3×10^{19} W/cm^2 is 1.5×10^8 cm/s. Similarly, the longitudinal velocity of the plasma jet from the rear side of a Cu foil ($n_0 \approx 85 n_{cr}$) irradiated at 10^{20} W/cm^2 is in the range 1–2 $\times 10^8$ cm/s, in reasonable agreement with the experimental observations. The density values used in the estimations above correspond to single ionization of Al and Cu, i.e. we assume moderate heating of the bulk target during the interaction.

7. The scaling of ion acceleration in the RPDA regime

The general requirements for the parameters of a laser accelerator are essentially the same as those for standard accelerators of charged particles [11], i.e. they should have a reasonable acceleration scale length, a high enough efficiency and the required maximal energy, a high quality, emittance and luminosity of charged particle beams.

Using the above obtained expressions for the ion energy dependence (11) on the laser pulse amplitude and length we can write the fast ion energy scaling. In the nonrelativistic limit, when $\gamma_\alpha = \mathcal{E}_\alpha/M_\alpha c^2 \ll 1$, it is

$$\mathcal{E}_\alpha = 8 \times \left(10^{11}/N_{tot}\right)^2 (M_p/M_\alpha)(\mathcal{E}_{las}/1\ \mathrm{J})^2\ \mathrm{MeV} \tag{36}$$

Here M_p is the proton mass and N_{tot} is a number of accelerated ions. In the ultrarelativistic limit, $\gamma_\alpha \gg 1$, the scaling has a form

$$\mathcal{E}_\alpha = 6.25 \times \left(10^{11}/N_{tot}\right)(M_p/M_\alpha)(\mathcal{E}_{las}/100\ \mathrm{J})\ \mathrm{GeV} \tag{37}$$

The ion acceleration length in the limit $\gamma_\alpha \gg 1$ is of the order of

$$l_{acc} = l_{las}/(1 - v_\alpha/c) \approx 2\gamma_\alpha^2 l_{las} \tag{38}$$

As we see, the acceleration length depends on the laser pulse duration, τ_{las} ($l_{las} = c\tau_{las}$), and on the final energy of accelerated ions, $m_\alpha c^2 \gamma_\alpha$.

As an example, we consider a solid density foil, $n_0 = 10^{24}\ \mathrm{cm}^{-3}$, of 1 μm thickness irradiated by a laser pulse with a transverse size of 100 μm. For a laser pulse energy of the order of 200 kJ we find that the accelerated ion energy is equal to 1 TeV with a total ion number of 10^{12}. For a laser pulse duration of $\tau_{las} = 1$ ps, the pulse length is equal $l_{las} \approx 0.03$ cm. In this case for $\mathcal{E}_i = 1$ TeV the acceleration length is approximately equal to $l_{acc} \approx 0.6$ km. If we assume the laser pulse length to be 30 μm, i.e. $\tau_{las} \approx 100$ fs, and laser energy is equal to 20 kJ, protons achieve the energy about 100 GeV over the acceleration length of the order of 60 cm.

Parameter of fundamental importance such as the luminosity characterizes the number of reactions produced by the particles in colliding beams of a collider. The luminosity is given by the expression $\mathcal{L} = f(N_1 N_2/4\pi\sigma_y\sigma_z)$, where N_1 and N_2 are the numbers of particles in each of the beams, σ_y and σ_z are the transverse size of the beam in the y and z directions, and f is the frequency of the beam collisions. The product of the luminosity and the reaction cross section gives the reaction rate. We see that the luminosity can be increased by increasing the particle number in a bunch, N_j, and/or by increasing the repetition rate, f, or by decreasing the transverse size of the bunch, σ_i, by focusing the particle beam into the minimum size focal spot.

In order to achieve high values of the ion bunch luminosity it is highly desirable to decrease the transverse bunch size. This can be achieved by modulating the density inside the foil, e.g. by a properly modulated laser pulse. The analysis of the foil motion presented in Section 4 shows an exponential growth of the modulations. This opens the way for focusing the acceleration of ions onto a narrow spot with a lower limit given by the foil thickness. Using these results we can estimate the RPDA accelerated ion bunch luminosity as

$$\mathcal{L} = 10^{34}(f/1\ \mathrm{kHz})\left(N_{tot}/10^{12}\right)^2\left(10^{-4}\ \mathrm{cm}/\sigma_\perp\right)^2\ \mathrm{cm}^{-2}\,\mathrm{s}^{-1} \tag{39}$$

which is of the order of the luminosity of standard accelerators.

Acknowledgements

This work is partially supported by the Grant-in-Aid for Scientific Research (A), 20244065, 2008 from MEXT (Japan) and VITP-ELI.

References

[1] V.I. Veksler, At. Energ. 2 (1957) 427.
[2] G. Mourou, et al., Rev. Mod. Phys. 78 (2006) 309;
M. Borghesi, et al., Fusion Sci. Technol. 49 (2006) 412.
[3] M. Borghesi, et al., Plasma Phys. Controlled Fusion 5 (2008) 124040.
[4] T.Zh. Esirkepov, et al., Phys. Rev. Lett. 92 (2004) 175003.
[5] F. Pegoraro, S.V. Bulanov, Phys. Rev. Lett. 99 (2007) 065002.
[6] T. Esirkepov, et al., Phys. Rev. Lett. 96 (2006) 105001;
X. Zhang, et al., Phys. Plasmas 14 (2007) 073101;
T.V. Liseykina, et al., Plasma Phys. Controlled Fusion 50 (2008) 124033;
S.S. Bulanov, et al., Phys. Rev. E 78 (2008) 026412;
A. Robinson, et al., New. J. Phys. 10 (2008) 013021;
O. Klimo, et al., Phys. Rev. ST Accel. Beams 11 (2008) 031301;
M. Chen, et al., Phys. Plasmas 15 (2008) 113103;
V.K. Tripathi, et al., Plasma Phys. Controlled Fusion 51 (2009) 024014.
[7] S. Kar, et al., Phys. Rev. Lett. 100 (2008) 225004.
[8] E. Ott, Phys. Rev. Lett. 29 (1972) 1429.

[9] W. Manheimer, et al., Phys. Fluids 27 (1984) 2164;
T. Taguchi, K. Mima, Phys. Plasmas 2 (1995) 2790;
F. Pegoraro, et al., Phys. Rev. E 64 (2001) 016415.
[10] L.D. Landau, E.M. Lifshitz, The Classical Theory of Fields, Pergamon Press, Oxford, 1980.
[11] S. Humphries Jr., Principles of Charged Particle Acceleration, Wiley, New York, 1999.
[12] T. Esirkepov, Comput. Phys. Commun. 135 (2001) 144.